CRYOGENIC, HIGH SPEED, TURBOPUMP BEARING COOLING REQUIREMENTS

Fred J. Dolan, Howard G. Gibson, and James L. Cannon
Marshall Space Flight Center
Marshall Space Flight Center, Alabama 35812
and
J.C. Cody
SRS Technologies
Cummings Research Park West
Huntsville, Alabama

ABSTRACT

Although the Space Shuttle Main Engine (SSME) has repeatedly demonstrated the capability to perform during launch, the High Pressure Oxidizer Turbopump (HPOTP) main shaft bearings have not met their 7.5 hour life requirement. Since cryogenic bearing performance data in the literature was extremely limited, especially for bearings of SSME size and speed, a test program was initiated at the Marshall Space Flight Center (MSFC). A tester is being employed to provide the capability of subjecting full scale bearings and seals to speeds, loads, propellants, temperatures, and pressures which simulate engine operating conditions. The tester design permits much more elaborate instrumentation and diagnostics than could be accommodated in an SSME turbopump. Tests have been made to demonstrate the facilities; and the devices' capabilities, to verify the instrumentation in its operating environment and to establish a performance baseline for the flight type SSME High Pressure Oxidizer Turbopump Turbine Bearing design. Bearing performance data from tests are being utilized to generate: (1) a high speed, cryogenic turbopump bearing computer mechanical model, and (2) a much improved, very detailed thermal model to better understand bearing internal operating conditions. Parametric tests have also been made to determine the effects of speed, axial loads, coolant flow rate, and surface finish degradation on bearing performance.

As a result of past test data and failure analyses, the MSFC Bearing and Seal Materials Tester (BSMT) operations team's contention that the SSME HPOTP bearing problem was related to over temperature resulting from insufficient cooling, and the fact that this contention was further substantiated by the bearing thermal modeling effort being accomplished by SRS Technologies, management at MSFC directed the team to perform a series of bearing thermal limits tests. Two test series were planned; the first with Phase I bearings in LN_2, and the second with Phase II bearings in LOX. This paper discusses the results of the first test series which explored the effects of cryogenic fluid subcooling on the thermal stability of SSME high speed cryogenic bearings and their performance after encounters with thermal ex-

cursions. During this test series, two thermal instabilities and accompanying thermal excursions were encountered; one at a time in different tests. Both caused red line cutoffs and both were verified by borescopic inspections immediately after the test and at disassembly. With the bearing outer race temperature "red lines" removed, two additional tests were made to further explore bearing operating characteristics after thermal excursions and after wear had occurred. This test series has provided very good and convincing data, plus excellent hardware evidence, that the SSME HPOTP bearings are indeed being operated very near the point of thermal instability. Both borescopic evidence and evaluation (failure analyses) of the bearings at disassembly provided overwhelming evidence that they both had experienced thermal instability and (thermal) excursions. Both damaged bearings displayed visual degradation characteristics essentially identical to those noted in SSME developmental engine bearings.

Introduction

Although the Space Shuttle Main Engine (SSME) has demonstrated the capability of performing acceptably through twenty-four successful Space Shuttle missions at launch power levels of 100% and 104%; it has not met its 55 successive flights and 7.5 hour life goals. The performance and life of the High Pressure Oxidizer Turbopump (HPOTP) mainshaft bearings are one of the prime causes of this failure to meet life goals. Additional comments on the authors' position relative to this bearing problem are contained in previous papers pertaining to this subject, see References 1 and 2. Brief descriptions of past and present bearing problems and efforts made to improve these conditions, plus several prior test series and the results of those efforts are also contained in the above references.

Considerable controversy has existed between various different factions for several years relative to the cause or causes for these HPOTP bearing problems and changes required to materially improve these conditions. These factions have existed within the bearings, turbomachinery and analytical groups involved in this program. There were several factions each of which had a "favorite scenario" relative to what initiated the bearing wear mechanism. Although the problem and controversy have existed for years there had been no resolution to or agreement on this failure analysis dilemma. A major problem to the resolution of this dilemma was the fact that the faction in control of the program had misinterpreted the failure analysis evidence.

In spite of the fact that the BSMT operations team had contended that the problem was thermal and one which could be at least partially alleviated by improved cooling, no increased or improved cooling "fixes" were attempted, nor were thermal limits or thermal margin tests requested, planned, or made. Ultimately, however, an expressed concern for safety relative to temperature margin, i.e., between maximum bearing operating temperature and bearing material auto-ignition

temperature, resulted in management's decision to request that thermal margin tests be made such that this issue might be resolved.

In an effort to obtain the thermal margin data requested, the BSMT operations team began to plan a sequence of tests intended to produce data which could be used in conjunction with the analytical models previously developed (see References 3 and 4) to accomplish the desired result. the test plan was constrained/impacted to some degree by a lack of availability of Phase II turbine end bearings from the contractor, by the need to add another shaft seal at the drive end of the tester to address a safety issue, and to verify the new seal's proper operation in LN_2 before testing in LOX. Consequently, available Phase I bearings were scheduled for use and LN_2 was the planned coolant. For a description of Phase I and Phase II bearings see Table 1. Since the SSME HPOTP bearing problem was one of surface distress low in the inner race raceway in mild cases, and evidence of overheating (i.e., grey to black discoloration on balls and races) plus wear of both balls and races (low and high in the raceway) in the more severe cases, we continued to believe that the problem was one of marginal cooling. It was believed that this marginal cooling situation resulted in operation of the bearings very near the point of thermal instability, i.e., very near a point where the bearing thermal energy generated approached the maximum heat removal capability of available coolant. It was also believed that operation at or near the point of thermal instability could be created in one of these bearings by either (1) reducing the coolant flow rate to that minimum required to sustain a heat balance or (2) reducing the subcooling of the cryogenic fluid used to cool the bearing, i.e., cause the bearing's warmest areas to change over from liquid to vapor cooling thereby reducing the heat transfer coefficient and creating a thermal imbalance. Consequently, a test plan was generated which included not only reducing subcooling and then lowering the flow rate, but one which also proposed raising bearing loads (heat generation) should the first two methods not be enough to create the desired imbalance. It was desired to create a thermal instability and accompanying thermal excursion such that bearing outer race outside diameter temperature test data could be obtained with which modeling might be utilized to predict maximum ball and raceway temperatures. Bearing hardware would also be subjected to metallurgical analysis to establish maximum internal operating temperatures. These temperatures and the auto-ignition temperature of 440C bearing steel could then be compared to establish thermal margins. This test data has been generated with HPOTP Phase I bearings in LN_2 and preliminary modeling and metallurgical analyses of test bearing hardware have been completed.

Test Objectives

The following is a list of the MSFC Bearing and Seal Materials Tester (BSMT) objectives for this particular test series.

a. Determine the proximity of HPOTP bearing operating conditions to thermal instability in LN_2 by operating bearings in a coolant

environment similar to, better than and worse than that in the HPOTP while measuring operating characteristics such as coolant flow rates, pressures, temperature, displacements and accelerations.

b. Provide data to support a similar tests series with Phase II bearings using liquid oxygen as the coolant, i.e., generate new and unique LN_2 data at low subcooling values; supply that data to computer model SHABERTH and SINDA users for the purpose of assisting in the establishment of operating values for flow rates, pressures, loadings, and the "red line" cutoffs to be used during the LOX test.

c. Permit correlation of measured parameters with bearing modeling results and metallurgical evaluations for verification of the models' ability to predict thermal instability conditions, sensitivity to vapor generation, and other characteristics of interest internal to the bearings that cannot be measured.

d. Provide the opportunity to evaluate the SSME Helium Barrier Seal recently incorporated into the tester design and to assess its performance under operating conditions. In this application the seal was energized with (or supplied from) a gaseous nitrogen (GN_2) source.

e. Improve capability for contributing directly toward SSME and future engine bearing problem solving by expanding knowledge and understanding of cryogenic bearing operation and behavior.

Test Facility

The facility being utilized includes a hazardous, remotely operated test stand with drive train, propellant supply and control systems as well as the bearing and seal materials tester itself. Fortunately, a test stand was available which had the required liquid oxygen, LO_2, (or LN_2) and liquid hydrogen tank volumes and pressure ratings which would be necessary to support the flow rate and test durations anticipated.

An artist's concept of the test facility referred to is shown in Figure 1. In this figure a large, low pressure LO_2 (or LN_2) storage tank (Dewar) can be seen in the lower left hand side of the view. Above that is the high pressure LO_2 sphere called the run tank; a 2,000 psi, 3,000 gallon pressure vessel. To the right of the LO_2 run tank are a building which houses the tester drive system and an instrumentation trailer. Progressively to the right are the test stand superstructure and a LH_2 storage Dewar.

Since this test facility had already been used for Space Shuttle Solid Rocket Booster Thrust Vector Control System testing and small propulsion systems tests, required cryogenic tankage and instrumenta-

tion channels existed at the remote site. Essentially the only new equipment required was a drive system with a building to house it, a tester mount, plumbing to supply propellants, and instrumentation peculiar to the tester, and its propellant lines. A photograph of the test facility is shown in Figure 2. From left to right are: the high pressure (2000 psi) propellant tanks, a building containing the drive system with adjoining shed to cover the tester and its mount, plus an instrumentation trailer. The test stand in the background is not used for this project. Figure 3 is a schematic diagram of the test facility showing plumbing and selected instrumentation. Figure 4 is a photograph inside the drive system building showning the 455 HP turbocharged diesel engine, plus a small portion of the fluid drive (speed controller) mechanism in the lower right hand corner. Figure 5 is another photograph taken inside the building; this one, however, shows a better view of the fluid drive mechanism, a non-contact speed and torque sensor, plus a gearbox that increases speed by 22:1 and a one inch thick steel plate blast wall. The tester is just on the other side of the blast wall. Figure 6 is a photograph of the cryogenic bearing and seal materials tester fully installed in its test position. Also shown are its mounting mechanism, propellant delivery and removal systems, and some of the instrumentation being utilized. Figure 7 is a photographic view of the other (left hand) side of the tester showing additional instrumentation and plumbing details.

Figure 8 is a cross sectional view of the tester's internal configuration. From left to right are the drive (quill) shaft, the tester with its shaft, bearings and seals, and the axial load cylinder on the right hand end. The new (SSME HPOTP) helium barrier seal is mounted on the right hand side of the left end plate. Its mating surface is a flange on the right hand end of the quill (drive) shaft. The shaft seals shown outboard of each bearing pair are primary oxidizer seals from the SSME HPOTP. They are actual flight hardware as are the bearings, the seal supports, and certain other lesser items of this assembly. Three axial loading mechanism push rods at 120° increments apply force to the outboard bearing carrier which, because of the carrier and spring design, actually supplies additional axial load (in addition to the preload) across the two inboard bearings while the outboard bearings' preload springs are partially unloaded by the relative motion between shaft and carriers. All of the bearing carriers are free to slide in the housing bore; however, the one on the left is restrained by three cylindrical, radial pins, plus when axial load is applied, the left hand (#4 bearing) carrier is designed to bottom and bear against the stationary seal support and housing bulkhead to its left (drive end). Bearing carriers are pinned to prevent rotation; however, the dowel pin hole on one end of each pin is slotted to permit the motion required by radial loads.

Tester Assembly and Balancing

In order to assure that contamination is not an uncontrolled variable, all parts are cleaned per MSFC-SPEC-164 for liquid oxygen

service prior to assembly; plus, cleanliness is maintained through assembly and balancing via the use of 100K clean rooms. Parts are double bagged for storage or transportation outside clean rooms. The rotating assembly is balanced on a Schenck Trebel dynamic balancing machine to less than 1.0 gram inch in each of two planes. Extreme care is taken via partial bagging and other means to prevent drill chips from entering the bearings during balancing, plus the assembly is recleaned after balancing and prior to its installation into the housing. Typical residual unbalance numbers have been 0.1 to 0.6 gram inch per plane. Figure 9 is a picture of the full scale model of the Bearing and Seal Materials Tester. This device has been used to train personnel in assembly and disassembly methods and procedures.

The assembly is subjected to pressure and leakage tests, plus a cryogenic torque test prior to shipment to the test stand. All assembly, balancing, test, installation, and instrumentation work is accomplished in accordance with detailed, written procedures.

Instrumentation Installation and Pretest Checkout

Subsequent to mechanical installation and alignment of the tester in the test stand external instrumentation is added, adjusted, and each channel subjected to an end-to-end systems check, i.e., a check from the instrument to the recording device. Each instrument is individually calibrated prior to its installation. Facility instrumentation is also verified for proper operation from end-to-end. After instrumentation installation is completed an ambient temperature pressure and leak test is accomplished. The signals from instruments utilized (briefly described on Figure 8) are recorded either on high speed data tape at rates up to 20 KHz or are stored in the memory of a computer. The slower frequency signals are scanned and recorded at 25Hz and recorded by a computer. (For a complete list of instrumentation please see Reference 2).

Subsequent to tester installation, alignment and instrumentation, cold shock, leakage, and cold flow tests were made to verify proper operation of system controls and instrumentation.

Test Procedures

Prior to each rotational test the cryogenic propellant supply system and the bearing tester are thoroughly chilled for in excess of two hours with a low pressure low flow rate chilldown procedure optimized experimentally early in the program. The bearing tester is not operated until it is throughly chilled, cold torque checks and cryogenic leak checks at pressure are completed, supply and internal pressures and the desired bearing coolant flow rate are established and stabilized. The tester is then brought up to speed utilizing the fluid drive speed control mechanism. The diesel engine would already have been brought up to speed. Tests are generally intended to last a scheduled period of time based on the test objectives; however, some

have been short, but a few have been long almost to the point of run tank depletion. An automatic shutdown system was incorporated to abort the test whenever one or more of the critical measurements exceeded a red line (maximum or minimum) value. Red line measurements and values are shown on the Instrumentation List which was included in the previously mentioned report (Reference 2).

Data Handling and Review

(A relatively complete description of data handling and review methods was also included in Reference 2).

Brief Test Review

Four test series have been completed. The first, a design certification and calibration (DCC), test was intended to demonstrate the facilities capability (including the tester) to meet certain design requirements, i.e., test conditions to be imposed on the bearings and seals in the tester. The second test series was intended to begin the characterization of the then current flight design SSME HPOTP turbine end bearing at a representative load. The results and analyses of both of these test series were reported in Reference 2. The third test series was one wherein a study was made concerning the feasibility of lubricating these cryogenic bearings with a LOX compatible oil (Krytox 143AZ) by vacuum impregnating the porous Armalon cages. The intent was to have a very thin oil film on the metal bearing parts, a film too thin to freeze the bearings while thoroughly chilled, but one thick enought to provide a lubricating film when rolling contact surfaces warmed above the oil's melting point (approximately -125°F) during normal operation. Methods were developed to vacuum impregnate the cages with a quantity of oil such that the bearings were lubricated at room temperature and yet not mechanically freeze or lock up when chilled to LN_2 temperature, or to LOX temperature in the case of the engine. The variables were controlled such that the bearings operated smoothly during balancing and other room temperature operations. They rotated easily when chilled to LN_2 temperature; however, during full speed "all up" operation of the tester in the normal mode, surface distress occurred earlier in the life of these bearings than it normally had with the standard dry film lubricant application. Surface distress began to appear on the balls at approximately 2400 seconds of operation with the oil lubrication; whereas it had required approximately 3200 seconds with dry film lubrication. The exact reason for this was not established; however, it is believed to have been at least partly a result of surface finish damage which occurred during the time of operation with frozen lubricant on the surfaces. A further contributing condition may have been a reduction in polytetrafluoroethylene (PTFE) transfer film lubrication from the cage to the balls and finally to the races. This reduction in PTFE transfer film may have been a result of frozen lubricant in and on the cage, or an upset of the surface characteristics which normally cause the transfer to occur, or both. Whatever the reason it was decided that that approach

to improved lubrication was not going to be developed quickly or easily and, in fact, appeared as though it might never work as originally intended. Consequently, that approach was put aside in order to perform the thermal limits testing previously discussed. The fourth test series, the subject of this paper, was intended to begin addressing the thermal limits issue. The results of this test series will be reported here.

Test Plan

In order to achieve the desired test objectives, as outlined previously, a rigorous test plan was developed. The test plan as presented in Table 2 focuses on the primary variables: reduced subcooling, flow rate, and applied axial load. These test variables would be changed one at a time in order to evaluate their influence on bearing performance. Subcooling was selected because test data in this area was insufficient and analysis of the HPOTP bearings showed subcooling to have significant effect on bearing performance. Previous parametric tests had focused on determining the effects of speed, coolant flow rate, axial load and surface finish degradation on bearing performance. These additional parametric studies were planned in case the desired thermal imbalance could not be created with reduced subcooling alone. Because of the severe bearing degradation experienced in this test series with reduced subcooling it was not necessary to implement those additional tests (parametric variables). Those additional variables will be the objectives of future tests.

Certain test parameters were held constant throughout this test series, things such as: tester speed at 30,000 RPM, flow rate at 4.6 lbm/sec, and applied axial load at 300 lbs. Tester speed and bearing coolant flow rate were selected in order to simulate the speed and flow conditions of the HPOTP turbine end bearings. The 300 lbs axial load was applied to compensate for the density change that would be experienced when the coolant is changed from LN_2 in the current test series to LOX for the next test series. The fluid density change between LN_2 and LOX affects the parasitic loads on the bearings as a result of the pressure drop across the bearings. By maintaining equivalent loads on the bearings, the heat generation should be approximately the same for both test series. The total steady state axial load on inboard Bearings Two and Three is approximately 2500 lbs which is the sum of the applied axial load, bearing preload (1000 lbs), and the parasitic load (1200 lbs). From a comparison standpoint, loads experienced by the tester bearings are not representative of the steady state loads experienced by the HPOTP bearings with the exception of the bearing preload. In fact, the turbine end bearings experience relatively high fixed and dynamic radial loads during steady state operations and high axial loads only during transient operation. In preparing the test plan, the current tester limitation on controlling bearing loads was recognized and no attempt was made to simulate the HPOTP bearing loads.

After completing the preliminary checkout tests, the first formal test was run at the standard test conditions with approximately 43 degrees subcooling at the inlet to the bearings to establish a baseline condition. Subcooling of the fluid at the inlet to the bearings was controlled by the backpressure control valve in the discharge circuit. Subcooling as described here refers to the number of degrees away from the LN_2 saturation line at a given temperature and pressure. Subcooling at the inlet of each bearing pair was calculated based on the temperature probes located upstream of each bearing pair at the bearing pitch diameter. Pressures in the cavity upstream of the bearing pair were estimated from tester inlet pressure data and previous pressure probe data, see Reference 5.

Subsequent tests as summarized in Table 3 were a continuation of the subcooling tests where the back pressure was decreased in order to drive the fluid subcooling toward the LN_2 saturation line. Figure 10 illustrates the technique employed in reducing the tester internal pressure in increments to achieve the desired subcooling. Based on the results in the fifth test, N2451RDB, where the test was started with poor subcooling (17 degrees) and the number two bearing outer race temperature red line cut terminated the test just after reaching 30,000 RPM, it was decided to start the remaining tests with a large subcooling margin and then drop the backpressure to the desired subcooling level to better assure that thermal equilibrium was achieved.

Test Results

During this LN_2 test series, valuable data was obtained on the sensitivity of the 57mm bearing to changes in coolant pressure an subcooling. Several significant events were encountered in these tests such as the two thermal instabilities and subsequent thermal excursions as well as the continued performance of these bearings after experiencing a thermal excursion. This bearing thermal data provided the necessary correlation with the bearing model results and permitted calibration of the bearing thermal model.

Results from this test series can be readily summarized relative to significant test events. The first thermal excursion occurred in Bearing Number Two on test N2451RDB when the test was started with approximately 17 degrees subcooling at the bearing inlet. As the tester reached 30,000 RPM the Number Two Bearing outer race thermal couple spiked exceeding the red line limit of -200°F, thus terminating the test. Maximum bearing outer race temperature during this excursion was -125°F as shown in Figure 11. After this test, the red line limit on Bearing Number Two outer race temperature was removed to permit observation of the bearing thermal behavior after experiencing a severe thermal excursion.

Thermal instability on inboard Bearing Number Three occurred on the seventh test, N247RDB, when the back pressure to the tester was reduced incrementally to 200 psi as shown in Figure 12. Subcooling at

the inlet to the bearings was 21 degrees when the maximum Number Three Bearing outer race temperature of -194°F occurred. This temperature violated the -200°F red line limit which terminated the test as shown in Figure 13. However, it should be noted that the Number Two Bearing, which went through a previous thermal excursion, operated at elevated temperatures, but did not experience an additional thermal excursion with reduced subcooling.

On the ninth and final test in this series, N2493RDB, the back pressure was varied to develop subcooling conditions ranging from 40 degrees down to 0 degrees in steps. Neither Bearing Two nor Three, as shown by the outer race temperature measurements in Figure 14, experienced any additional thermal excursions during this test, but continued to operate at elevated temperatures.

Results from this test series strongly suggest that bearings can experience thermal instabilities/excursions without catastrophic results. It was also inferred that these bearings experienced their maximum surface temperatures during these excursions. Temperatures experienced by the bearings during these excursions reduce the bearing internal clearance, contact angle, and material properties (a result of poor hot hardness capability) while increasing the contact stresses. This thermal/mechanical interaction must precipitate wear because on subsequent tests these bearings recovered and operated at elevated temperatures until excessive ball wear or cage failure occurred. As bearing wear increased, the bearing internal clearances and contact angles increased which made it much more difficult to induce a second thermal excursion.

This important information provided a significant link between tester data and results, and the bearing computer model. Prior to running this test series, the bearing tester computer model had been utilized to provide predictions of how the bearings would operate under various subcooling conditions. One example is shown in Table 4. Model predictions show the bearings to be thermally unstable between 15 and 13 degrees subcooling. Thermal excursions in Bearings Two and Three occurred at 17 and 21 degrees subcooling. This degree of agreement between the empirical data and the computer model is an extremely important event considering the complexity of the bearing mechanical and thermal models. Validation of the computer model has been a long and arduous task. It appears that this analytical tool has gained the maturity required to confidently evaluate future HPOTP bearing design changes as well as advanced turbopump bearing designs.

Application of the tester data and computer model were extended to predict the operating conditions of the HPOTP Phase II bearings to be tested in LOX and make predictions of the operating conditions of the HPOTP preburner pump and turbine end bearings. The predicted operating region of the HPOTP bearings, as indicated by the vertical bars, is shown in Figure 15. This graph illustrates the lack of cooling margin for the pump end bearings and only a limited amount of margin for the

turbine bearings. Based on current test data and modeling, a subcooled enthalpy of 25 to 30 BTU/LB could provide sufficient thermal margin for stable operation. Model results which previously showed the bearing to be unstable with reduced subcooling were updated to account for bearing wear which was measured upon tester disassembly. Results of this updated analysis, as shown in Figure 15, indicate the bearing would continue to operate which is similar to what was demonstrated in this recent test series. Based on current BSMT data which simulated the ball wear experienced in the HPOTP and the validation of the bearing computer model, it appears the current BSMT test program and modeling efforts have gained credibility by demonstrating the capability for testing, modeling, predicting, and understanding the operating characteristics of a complex high speed cryogenic bearing system.

Post Test Bearing Evaluations

At the conclusion of the test series, the tester was disassembled for evaluation of all internal hardware and replacement of the bearings. All internal tester parts, except for the bearings, were examined for condition and reusability in the clean room. Minor areas of dry film lubricant wear-through were noted in the inboard bearing carriers' (bearing) outer race locating bores. These conditions had undoubtedly been aggravated by considerable vibration and running time after the onset of bearing wear, but this set of carriers had been used through four test series without relubrication. The carriers were sent out for relubrication. The Kel-F HPOTP primary oxidizer seals were also noted to have encountered some wear. With bearing ball wear the position of the rotating part of the seal (with the laby teeth) undoubtedly moved axially with respect to the stationary Kel-F sleeves. These parts will be replaced for the next build. The bearings were removed from the clean room and taken to a laboratory for evaluation.

The two outboard bearings, numbers one and four, showed the least amount of wear and ill effects from reduced subcooling. These are the bearings that run with a lower axial load and those which the cryogenic liquid coolant enters first. The balls from these two bearings were shiny and smooth, with only a faint dull looking wear band. They were still round with very little or no wear. The races were only slightly worn. The outer races had no "negative angle," dark ball tracks, wear, nor surface distress, and little discoloration on the positive side. The inner races had more evidence of surface distress, more discoloration, but no major darkening. The wear tracks on bearing number one were faint and slightly roughened on both races. The wear track position on the number one inner race went from approximately 38° down to 4°. There was also a very very faint track (just a partial blending of the grinding matte finish) which extended from 4° down to approximately -4°. This track was attributed to balancing operations at room temperatures where, as a result of differences in the thermal coefficient of expansion between 440C bearing material and the Waspaloy shaft, a heavy press fit causes bearing internal clearance to be very small. There was very little discoloration associated with these races

indicating that thermally this bearing had been reasonably well behaved. The cage from this bearing was in excellent condition with light ball wear in the pockets. (Sketches of this and the other three bearings' post test conditions are included in Appendix A. Also see Figure 16.)

The number four bearing races were observed to have had more noticeable discoloration, particularly the inner race, plus the ball tracks were wider. The running track on the inner race extended from approximately 39° down the raceway face to approximately zero degrees where there was a blue band of discoloration. These attributes indicate that this bearing had been more advanced toward a thermal problem than the number one bearing. This bearing had not lost all its internal clearance as a result of a thermal gradient from the inner to outer race, but had clearly begun to suffer some preliminary ill effects from this condition. The cage ball pocket wear was noticeably heavier in this bearing than in the number one as well, although the cage was in good condition. Cage ball pocket wear is and has throughout the SSME program been a good sign that bearing ball loads had been amplified by the above described thermal effects (thermal gradient). Further discussion concerning this cage ball pocket wear variation as an indicator of bearing internal thermal conditions will be provided below. (Again, sketches of this bearing are contained in Appendix A. Also see Figure 17).

The cages of bearings one and four exhibited very light O.D. rubbing against the outer race lands and ball-to-cage contact 360 degrees around in the ball pockets. This ball-to-pocket contact was heaviest in the fore and aft directions of the cage with bearing number four having the greatest wear as previously mentioned.

The inboard bearings, numbers two and three, had the greatest amount of degradation and wear, with the number two being in the worst condition. It should be remembered that the number two bearing encountered a thermal instability and experienced a thermal excursion during the fifth test with approximately 17° subcooling and 885 seconds accumulated time on it; whereas, that same situation did not occur with the number three bearing until the seventh test with approximately 21° subcooling and 1285 seconds accumulated time. Consequently, the number two bearing was subjected to a good deal more operating time after the thermal incident had damaged the internal geometry and surface finishes. The two inboard bearings are expected to suffer the most damage in this tester because of a parasitic load caused by the pressure drop across the bearings exerting a force on the bearing carriers. This effect and its consequence was more completely discussed in Reference 2. As pointed out in Reference 2 this load has analytically been determined to be approximately 1200 pounds of additional load on the bearing carriers for bearings two and three at 4.6 pounds/second flow rate and 30,000 RPM. This parasitic load changes with both speed and flow rate.

Both bearing thermal excursions were sensed by bearing outer race temperature measurements and were truncated before they could proceed to completion. The emergency "red line" cut-off system caused both shutdowns. Borescopic inspections verified the existence of black balls in the subject (correct) bearings after tests five and seven. The remainder of the SSME HPOTP bearing failure characteristics were verified at disassembly. These test bearings' failure characteristics do, indeed, very closely resemble SSME HPOTP Phase II bearing failure characteristics which have been observed for the past approximately four or five years. These characteristics of thermal instability and thermal excursion are as follows:

(1) Very heavy load track low in the inner race raceway (caused by load amplification resulting from the loss of internal clearance and resulting reduced contact angle).

(2) Dark grey-to-black, worn balls.

(3) Worn, dark grey-to-black races.

(4) Ball track and wear extending to the negative (wrong) side of the outer race raceway (dark grey-to-black in color).

(5) Inner race thrust shoulder burr (caused by ball wear and ball to race contact moving up the raceway shoulder via centrifugal force as wear progressed).

Hardware examination via borescopic inspection between tests and later verification by teardown and analysis has shown these SSME characteristic traits. Borescopic inspection after Test No. 5 of Bearing No. 2 revealed that the balls were black, had moderate surface distress, and a few minor spalls exposing new, subsurface metal. The inspection of Bearing No. 3 after Test No. 7 showed similar results. The balls were grey to black in color, had mild surface distress in a band, and some minor spalling. Prior to these tests, these particular bearings had been in good condition, showing only slight banding and a dulling of the surface finish. The extent of the increase in temperature was limited by the red line values used to protect the tester. The bearing hardware inspection confirmed the occurrence of thermal runaway.

Bearing Number Two's outer race had a very wide contact area with both positive and negative angles, black surfaces, and grey surfaces with black "patches," minor spalling in the contact zones, and many small jagged, rough areas that protruded above the surface 360° around the race. These jagged, rough areas were oriented mainly in the axial direction. (See Figure 18). The inner race showed the same black banding with black "patches" low in the curvature, plus minor spalls and a rough surface texture low in the curvatures. There were many small jagged raised edges on the race in the axial direction similar to the outer race. These edges were in a shiny worn region. Ball contact

had been from very low in the raceway, approximately -7° to the upper shoulder which and been worn away approximately 0.02 inch and which had been rolled up in a burr at the raceway to shoulder intersection. This burr was very jagged and had some small sections (chips) missing. (See Figure 19). The cage showed signs of violent ball behavior after the thermal excursion. The webs between six ball pockets had been broken out with loose fibers and fragments still attached between the pockets. There was cage delamination in other ball pockets in regions of very heavy ball contact. Many of the remaining ball pockets were out of round, a result of heavy ball loads or high impact loads between the balls and cage pockets in the circumferential direction. Metallic particles were found imbedded in the O.D. of the cage around the ball pockets and the cage showed evidence of heavy rubbing against the outer race lands. (See Figure 20). The bearing balls were out of round and were worn from 0.0129 inch to a maximum of 0.0366 inch in a groove on the worst worn ball. (See Figure 21). The balls were black in color, but a few had a slight gold to brownish tint mixed in. It was observed during the borescopic inspections that the balls of Bearing No. 2 were a dark black after Test Five, but as more tests were conducted, the surface "lightened up" somewhat, indicating that the original degraded surface was being worn away. The balls also had very small to moderate skid marks and flat spots, plus some appeared to have "patches" of metal smeared on their surfaces. One particular ball had a groove worn around it approximately one-eighth inch wide indicating that it had rubbed against another ball with a great amount of force. This condition had been observed during the borescopic inspection after Test Number Nine. (See Appendix A for sketches of this bearing.)

Bearing Number Three had also experienced a thermal excursion during the test series, but the extent was limited by the red line cutoff. On inspection of Number Three, it was found to have similar characteristics as No. 2, but not as severe. The outer race had a very wide contact area with both positive and negative contact angles, bluish-black wide bands of color along with some smooth shiny appearing bands, and a black, slightly distressed, roughened band in the normal contact zone. (See Figure 22). The inner race had a region of minor to moderate spalling 360° around, low in the curvature. This region also had some metal smearing and was silver in color. This band was bounded on both sides with narrow, black, slightly roughened regions. The lower edge of ball contact extended from approximately 0° to the upper edge chamber. The upper region of curvature had a narrow, black band where the balls had been both rolling and skidding. The upper raceway to shoulder intersection had been rolled up in a burr which also had small segments (chips) missing. The shoulder width had been worn away approximately 0.01 inch. (See Figure 23). The cage pockets showed heavy rubbing fore and aft with some pockets having deep depressions in these directions. Some of these depressions had caused delamination to start occurring in an adjacent pocket along with a bulging out on the I.D. of the cage. A total of five ball pockets had a noticeably greater amount of wear than the other eight. One of the five had a lesser amount of wear than the others, but one had a much,

much greater amount of wear than the others. This variation in wear scar size from pocket-to-pocket in a single bearing cage has frequently been noted in bearings removed from SSME developmental engines. This trait is considered significant; more below. All the pockets were deformed to some degree in an egg shape. The O.D. of the cage had moderate rubbing indications in the outer race land piloting regions. (See Figure 24). The bearing balls varied in color from goldish brown to dark grey-black. Many of the balls had an orange peel surface with criss crossing wear bands with skid marks in the bands. Some balls had goldish brown areas covering one-half of the surface with metal distress in the region. A few of the balls had small "patches" of black metal on the surface along with an equatorial wear band which also had surface distress. The balls were worn from a low of 0.0047" to a maximum of 0.01" and were out-of-round. (See Figure 25.)

A variation in ball pocket wear scar size was mentioned above. This characteristic has been noted in SSME bearings which were worn, but has also been noted to a lesser degree in bearings which were not appreciably worn, but which showed evidence of thermal distress. This condition has been verbally discussed on several occasions, but was not pursued. It will be here in the form of a postulated reason for some variability in the cooling requirements at the onset of thermal instability. This is essentially an attempt to address why a marginally cooled bearing might operate satisfactorily in one test then have a problem in the next, or why one bearing might encounter this problem early in its life and another later, or not at all.

This scenario essentially proposes that uneven ball pocket wear is an indicator of non-uniform ball-to-cage loads, non-uniform ball heating and in the case of partially vapor blanketed balls, a method by which a few of the balls (3 to 5) may become significantly warmer and consequently larger in size than the other balls in that same bearing. Should this happen, and it appears to do so in some bearings, it is relatively easy to understand that individual difference in ball sizes would cause ball load and speed variations which would result in even larger cage loads and higher heat generation. This situation would be expected to rather quickly result in a serious aggravation of an already marginal thermal condition. It appears reasonable that a condition such as this, after it progressed beyond a certain point, would ultimately result in thermal instability and thermal excursion in these marginally cooled bearings.

This scenario is further explained as follows: The balls being used in these precision bearings are AFBMA (AntiFriction Bearing Manufacturers Association) Grade 10, meaning that they are spherical within 10 millionths (of an inch) and, within a bearing, are within 10 millionths inch of the same diameter. When one considers that our coefficient of friction tests of Armalon versus 440C in room air and in LN_2 have yielded results from 0.15 to 0.35 and that an average ball temperature difference of 3°F will result in a 10.2 millionths diameter variation (a 10°F temperature difference will result in 34 millionths

size variation), it appears that ball-to-cage load variation and the resulting temperature differences ball-to-ball could become very significant as ball wear surface temperatures exceeded coolant saturation conditions (temperature). Even though ball average temperature variations from cage load differences may be small when cooling is by the liquid, it is believed that this changes dramatically once the wear band temperature on the balls crosses the saturation line and vapor cooling of at least part of each ball begins. A significant heat increase at this point, even though it may be in the form of a relatively short transient, could cause a larger area on a ball to cross over from liquid to vapor cooling. Since at constant speed and load this is an irreversible process, liquid cooling would not return to those areas even though the loads were transient, in fact subsequent transients could cause even larger areas on those few balls to become vapor blanketed. As larger ball areas become vapor blanketed their diameters become larger causing them to run at a different speed than other balls in the bearing causing higher heat generation. This process is self reinforcing and will not reverse during operation because once the crossover to vapor cooling occurs it is followed very quickly by a ten fold delta temperature increase between ball track and coolant (vapor). This process can ratchet forward, but not backward; consequently, the process can only stagnate, or proceed until damage to the bearing results. Reversal from vapor to liquid cooling is not expected to occur in these bearings since heated tube heat transfer data showns that in order to revert from vapor back to liquid cooling a large decrease in heat rate and a large increase in coolant flow is required. The coolant is not expected to change, but the heat rate should rise as individual ball size and loads increase.

Some details from Bearing Number Three were submitted to metallurgy for evaluation. Metallurgical analysis of three balls which appeared to have been the hottest have been sectioned and subjected to microstructural evaluation and microhardness testing. It was found that a shallow surface layer was three "Rockwell C Scale" points harder than the substrate material. This has been interpreted to mean that the surface had been elevated to a temperature of approximately 1800°F during operation and that a quenching action must have occurred in LN_2 at shutdown to create surface material which was harder than the original substrate. Other samples have been submitted for Auger surface analysis, but results are not currently available.

Conclusions

From the results of tests conducted, data obtained, analyses made with that data, associated bearing modeling done in support of these tests and bearing examinations made both during and after the test series, the following conclusions have been drawn:

(1) With test conditions as similar to those in the SSME HPOTP turbine end bearing as practical, thermal instabilities were caused to occur by reducing fluid subcooling.

(2) These thermal instabilities occurred at subcooled values of 17° and 21°F in bearing numbers two and three respectively.

(3) Both bearing thermal instabilities were verified in the test data as well as in the disassembled hardware.

(4) When the threshold of adequate cooling was encountered a thermal excursion occurred very rapidly and without warning from existing BSMT instrumentation.

(5) As wear caused increased internal operating clearances and contact angles, thermal excursions were found to be much more difficult to induce in these bearings.

(6) The degraded bearings produced by these tests were noted to be essentially identical to those damaged bearings which have been removed from developmental SSME HPOTP's.

(7) Since the thermal stability threshold subcooling values determined were at or very near those considered normal for the SSME HPOTP turbine end bearing coolant source, this strongly suggests that these bearings have little or no margin relative to the balance between heat generation and heat removal (rejection) in the engine turbopump environment.

(8) Although neither of the thermal excursions encountered in these tests were allowed to progress to completion, the data and subsequent operational experience suggest that these bearings can experience thermal excursions without catastrophic failure, can recover and can continue to operate (with a greatly increased wear rate) until excessive wear and/or cage failure eventually occurs.

(9) Data suggests that the highest surface temperatures probably occur during the peak of the thermal excursion, that the chance of stopping a turbopump at the peak of this brief cycle is probably very slim, and that this high temperature evidence is undoubtedly worn away by subsequent operation (at the high wear rate condition).

(10) Testing in highly filtered LN_2 has demonstrated the capability to produce data and bearing failure conditions reasonably close to those generated in LOX (LO_2)

(11) It has been noted during testing in LN_2 that bearing outer race temperature measurements are much more volatile indicators of bearing cooling/thermal conditions than appears to be the case in LOX. For this reason it appears that testing in LN_2 has merit regarding the establishment of thermal margins and required/optimized coolant flow rates for desired bearing operating conditions.

(12) One of the conclusions drawn in Reference 2 was as follows: "Tests made indicate that the bearing and cooling system design tested was very marginal from a thermal management standpoint. Reduced friction and/or improved lubrication and cooling are necessary." This comment referred to the margin between operating conditions and thermal instability. These tests further reinforced those previous convictions.

(13) A variation in ball pocket wear scar size was noted in Bearing Number 3. This condition was similar to those noted in SSME HPOTP bearings. Since it is believed that this characteristic is very likely indicative of the wear process or may well suggest a key to the initiation of that process, a wear scenario has been developed based on this and other worn bearing characteristics, bearing operating conditions, and cryogenic fluid heat transfer characteristics which exist in the SSME HPOTP.

(14) Operational experience with the bearing tester in LN_2 and the test data generated have provided the training and data base needed for future tests in LO_2 with HPOTP Phase II bearings and with bearings of improved materials designs and lubrication characteristics.

References

1. Past Performance Analysis of HPOTP Bearings, B.N. Bhat and F.J. Dolan, NASA Technical Memorandum, TM-82470, March 1982.

2. MSFC Cryogenic Turbopump Bearing Tester Results and Analysis, F.J. Dolan and J.C. Cody, AIAA Paper presented at AIAA/ASME/SAE/ASEE 22nd Joint Propulsion Conference, June 1986, VBCC, Huntsville, AL.

3. Advanced Rocket Engine Cryogenic Turbopump Bearing Thermal Model, J. Cody, L. New, B. Tiller, Advanced High Pressure O_2/H_2 Technology Conference, June 1984, MSFC, Huntsville, AL.

4. Thermal Analysis of SSME Turbopump Bearings, J. Cody, D. Marty, and B. Tiller, 1986 Conference on Advanced Earth-to-Orbit Propulsion Technology, May 13, 1986, MSFC, Huntsville, AL.

5. BSMT LN_2 DCC Test Series Final Report, BSMT Review Team Members Assessment, S.A. Lowry, MSFC Internal Report EP 26 (85-100), dated June 27, 1985.

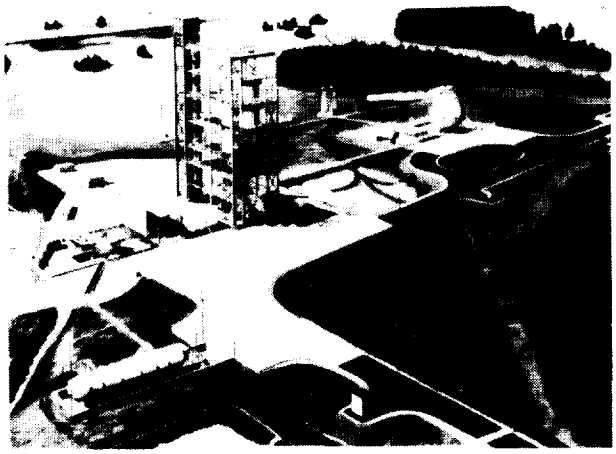

Figure 1. Artist Concept of Test Facility

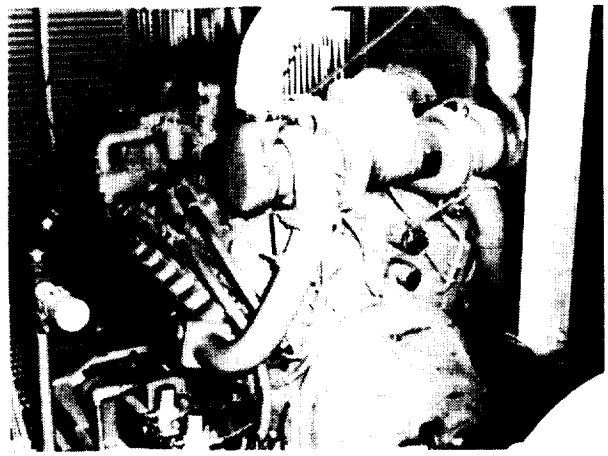

Figure 4. Turbocharged Diesel Drive Engine

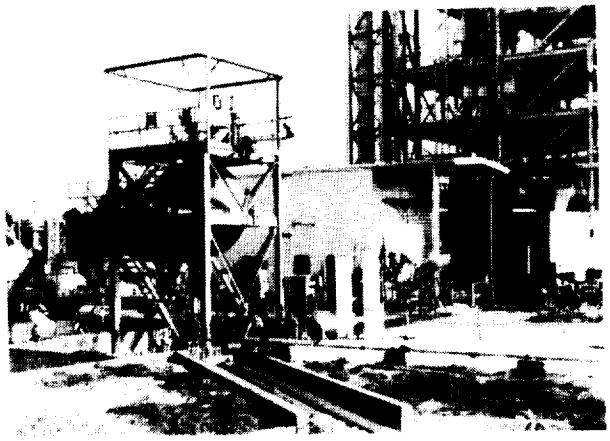

Figure 2. Test Facility

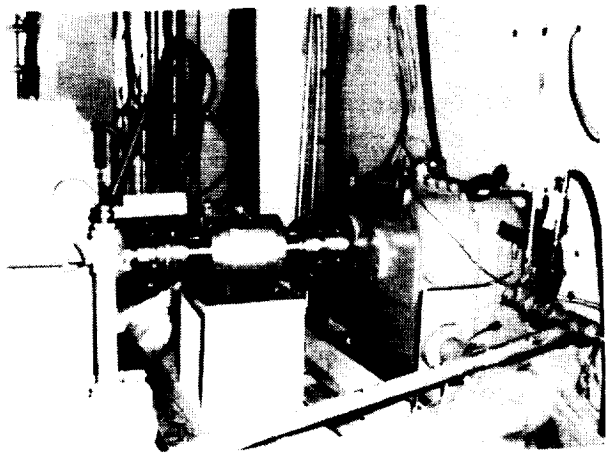

Figure 5. Drive Train Components

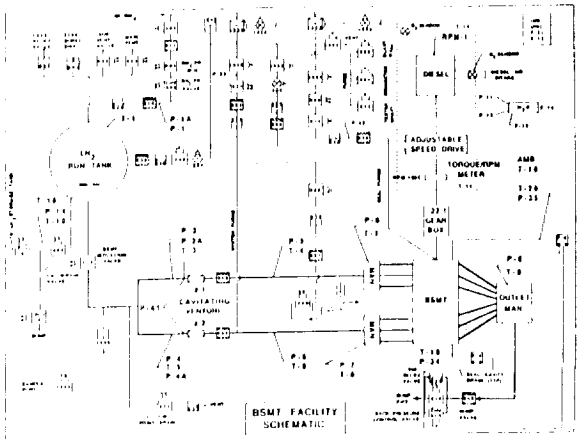

Figure 3.

Figure 6. Installed Bearing and Seal Materials Tester

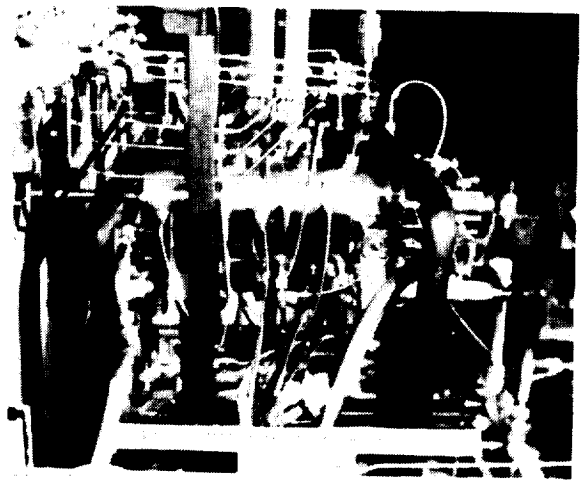

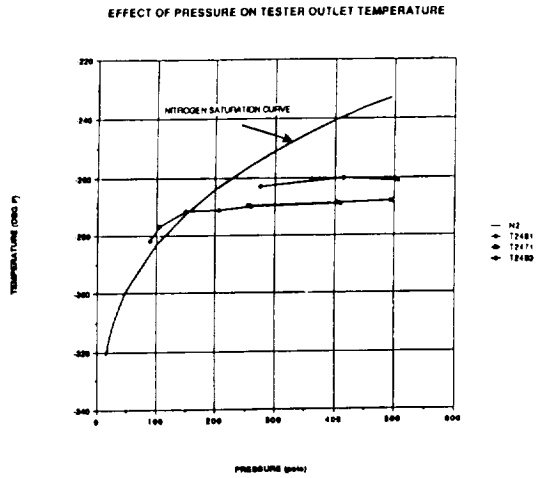

Figure 10. LN_2 Saturation Curve

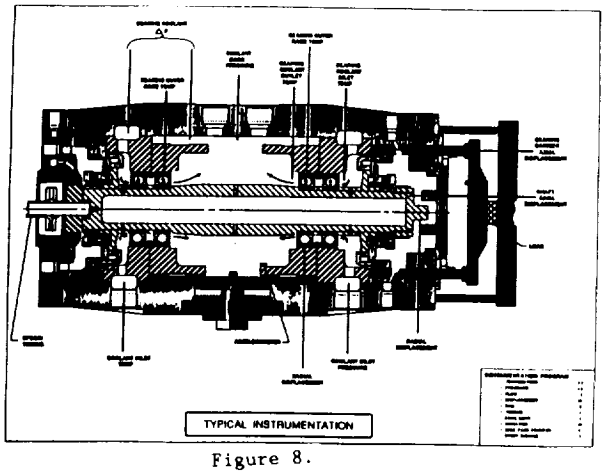

Figure 8.

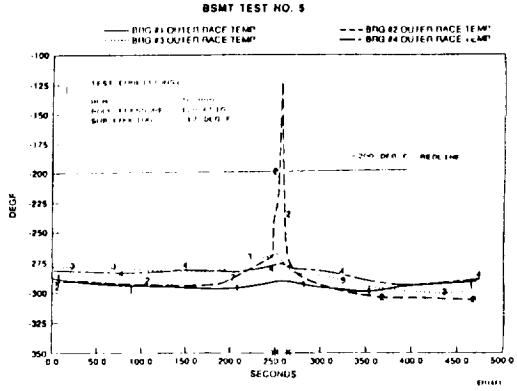

Figure 11. Outer Race Temperatures

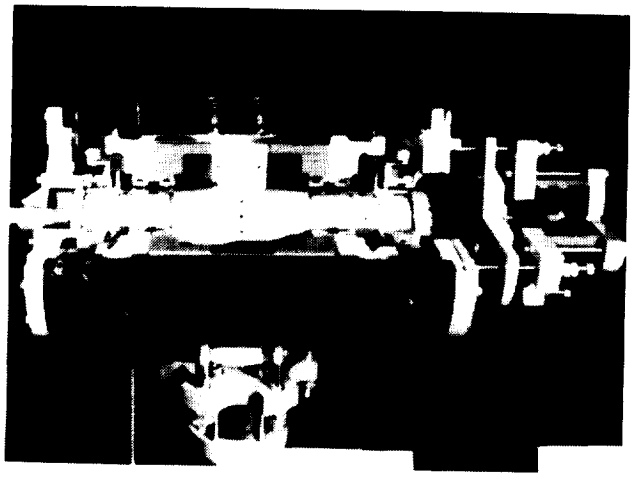

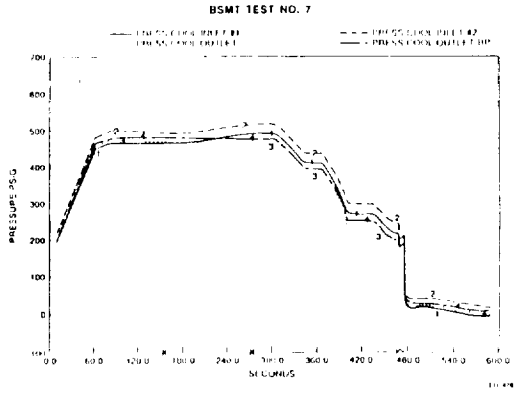

Figure 12. Pressure Step Down Curve

ORIGINAL PAGE
BLACK AND WHITE PHOTOGRAPH

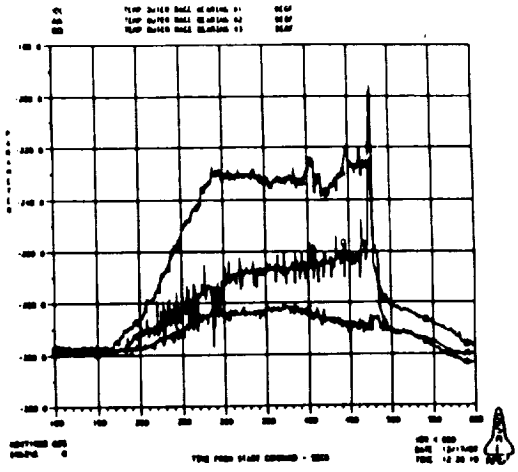

Figure 13. Outer Race Temperatures
Test No. 7

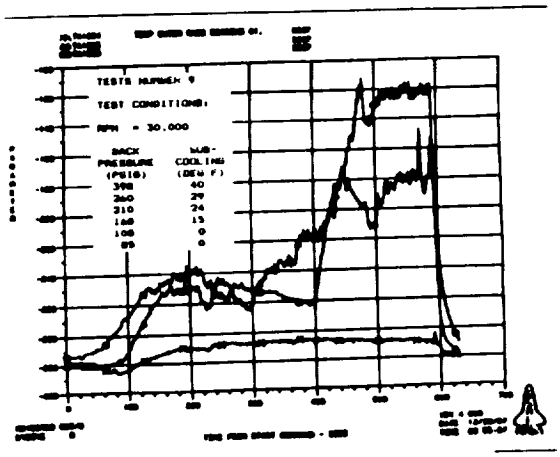

Figure 14. Outer Race Temperatures
Test No. 9

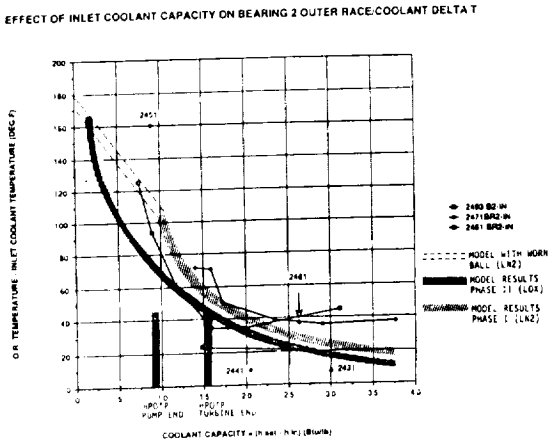

Figure 15.

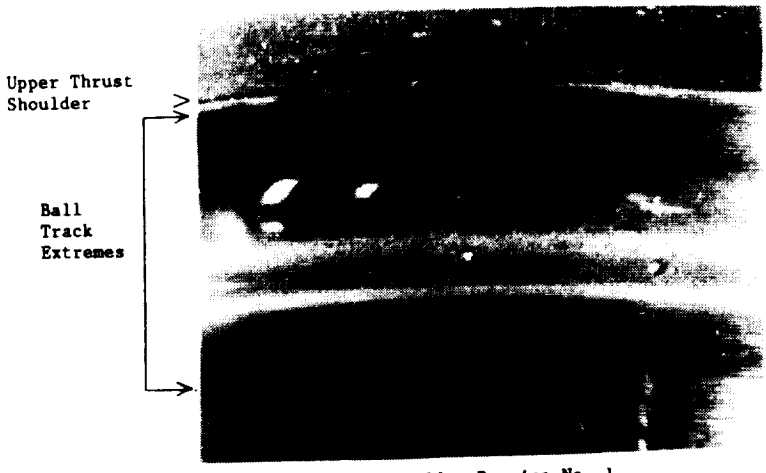

Figure 16. Bearing No. 1
Inner Race

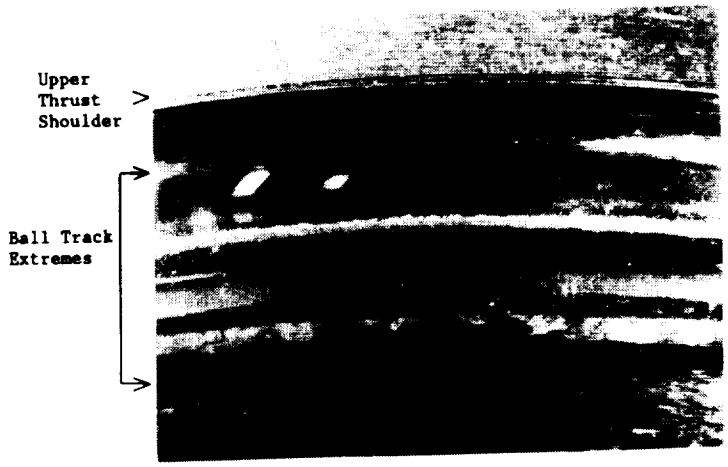

Figure 17. Bearing No. 4
Inner Race

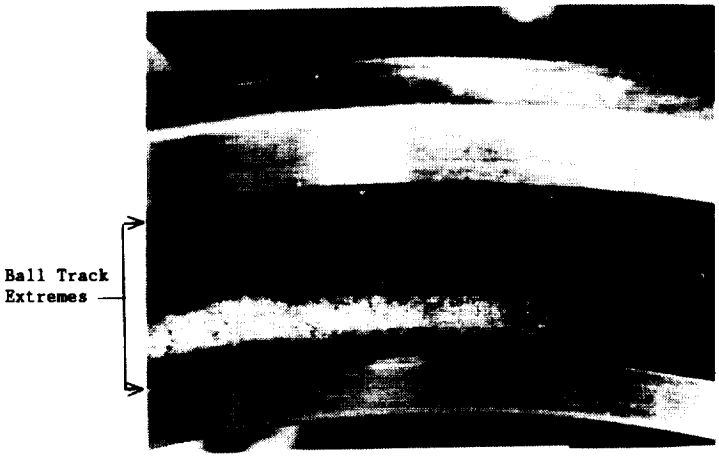

Figure 18. Bearing No. 2
Outer Race

Figure 19. Bearing No. 2
Inner Race

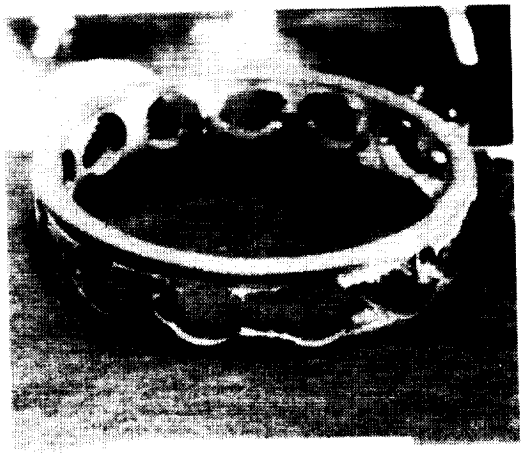

Figure 20. Bearing No. 2
Cage

Figure 21. Bearing No. 2
Balls

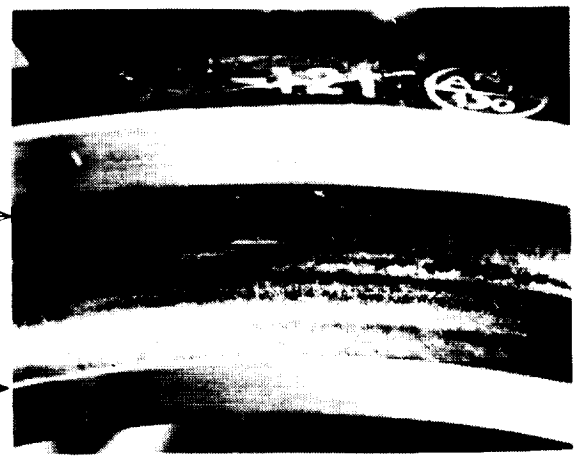

Figure 22. Bearing No. 3
Outer Race

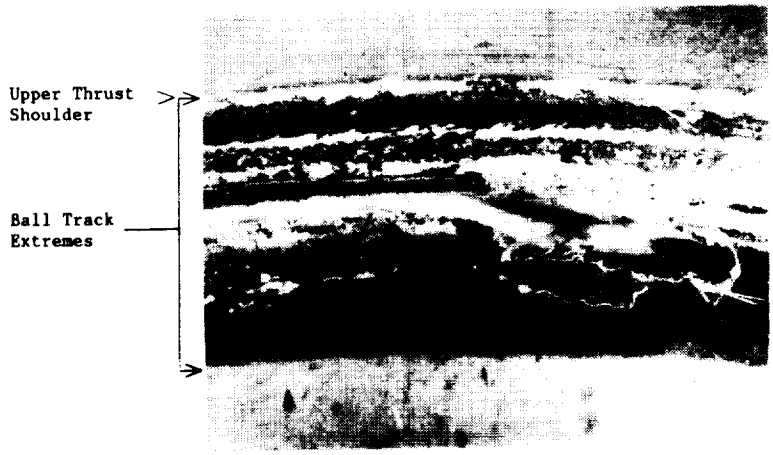

Figure 23. Bearing No. 3
Inner Race

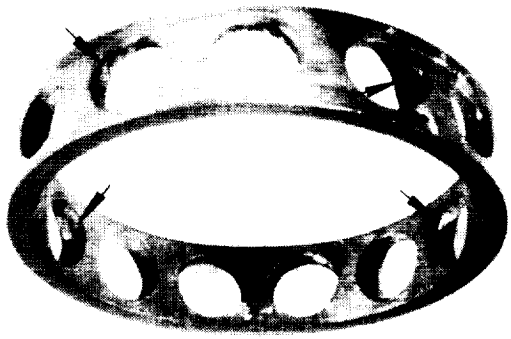

Figure 24. Bearing No. 3
Cage

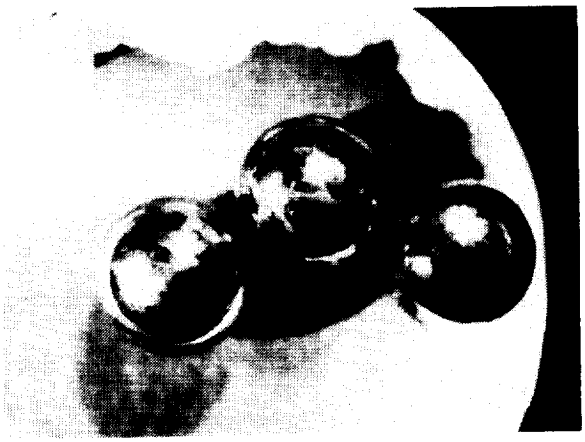

Figure 25. Bearing No. 3 Balls

57 MM BEARING COMPARISON CHART

	PHASE I	PHASE II
OUTSIDE DIA	4.06"	4.06"
BORE	2.25"	2.25"
DIAMETRAL CLEARANCE	.0036/.0040	.0059/.0063
OUTER RACE CURVATURE	53%	53%
INNER RACE CURVATURE	53%	55%
UNMOUNTED CONTACT ANGLE	20.5	22.5
MATERIAL	440C	440C
BALL SIZE	.500"	.500"
CAGE MATERIAL	ARMALON	ARMALON

Table 1

TEST PARAMETERS SPECIFIC TO INDIVIDUAL TESTS

TEST ID	RPM (K)	FLOW (LBM/SEC)	SUB COOL	VENTURI SIZE (INCH)	VENTURI INLET PRESS (PSIG) (PB/Pc)	TESTER INLET PRESS (PSIG) (P1001/P1000)	TESTER BACK PRESS (PSIG) (P1002/P1000)	TOTAL AXIAL LOAD (PA + APPLIED) (LBS)	PA LOAD (LBS)	APPLIED AXIAL LOAD FORCE (LBS)	APPLIED AXIAL LOAD HYD CYL PRESSURE (PSIG) (P1B)	TEST TIME (SEC)
M2431RDB	0	4.0	38°	.224	722	420	300	NONE	NONE	NONE	0	120
M2441RDB	10	4.0	48°	.224	722	400	300	870	870	NONE	0	30
M2451RDB	30	4.0	30°	.224	722	420	300	1500	1200	300	90	120
M2441RDB	30	4.0	30°	.224	722	300	300	1500	1200	300	90	120
M2491RDB	30	4.0	10°	.224	722	300	170	1500	1200	300	90	120
M2491RDB	30	4.0	8°	.224	722	195	195	1500	1200	300	90	120
M2471RDB	30	2.2	0°	.200	300	195	195	1500	925	575	60	120
M2491RDB	30	2.2	0°	.200	300	195	195	2000	925	1075	190	120
M2491RDB	30	2.2	0°	.200	300	195	195	2000	925	2075	311	120
M24191RDB	30	3.4	30°	.200	827	310	302	2900	1000	1420	172	120
M2411RDB	30	3.4	30°	.200	827	310	302	3500	1000	2420	302	120
M2491RDB	30	3.4	30°	.200	827	310	302	4500	1000	3420	413	120
M2491RDB	30	4.0	30°	.224	722	300	300	2500	1200	1300	157	120
M2441RDB	30	4.0	30°	.224	722	300	300	3600	1200	2300	278	120
M2491RDB	30	4.0	30°	.224	722	300	300	4500	1200	3300	399	120

Table 2

TEST MATRIX

TEST ID.	RPM	SUB-COOLING (deg F) DRIVE	LOAD	EXIT	BACK PRESS.	ELAPSED TIME ON BEARINGS	TEST DATE
M2431RDB	30 K	45	43	28	392 PSIG	380 SEC	25-NOV-87
M2443RDB	30 K	38	34	20	260 PSIG	620 SEC	25-NOV-87
M2451RDB	30 K	17	17	0	120 PSIG	700 SEC	01-DEC-87
M2461RDB	15 K	N/A	N/A	N/A	400 PSIG	900 SEC	03-DEC-87
	30 K	N/A	34	21	405 PSIG		
M2471RDB	30 K	S.C.	S.C.	--	485 PSIG	1310 SEC	10-DEC-87
	30 K	38	42	29	400 PSIG		
	30 K	26	31	18	260 PSIG		
	30 K	21	21	12	210 PSIG		
M2481RDB	30 K	S.C.	S.C.	--	480 PSIG	1640 SEC	15-DEC-87
	30 K	32	35	21	393 PSIG		
	30 K	22	25	9	243 PSIG		
	30 K	20	24	8	262 PSIG		
M2493RDB	30 K	40	43	28	398 PSIG	2190 SEC	18-DEC-87
	30 K	29	32	16	260 PSIG		
	30 K	24	27	11	210 PSIG		
	30 K	15	20	5	160 PSIG		
	30 K	0	17	11	108 PSIG		
	30 K	0	16	0	85 PSIG		

15,000 rpm rotations not shown

Table 3

BSMT COMPUTER MODEL RESULTS

Subcooling at Outboard Bearing (°F)	Outboard Bearing Inlet Pressure (psia)	Average Ball Temperature (°F)	Average Inner Race Temperature (°F)	Average Outer Race Temperature (°F)	Maximum Ball Track Ring Temperature (°F)	Outer Race Back Surface Temperature (°F)
38	485	-48	-134	-256	247	-252
35	440	-19	-126	-252	268	-245
30 *	385	59	-99	-240	345	-226
29	375	72	-92	-238	359	-223
21	300 *	150	-58	-226	451	-204
16	260	233	-17	-199	558	-166
13	235	*	*	*	*	*

Flow Rate = 4.6 lb/sec

Outboard Bearing Inlet Temperature = -272 °F

Pressure Drop Across Bearing Pair = 35 psia

Coefficient of Friction = 0.20

Inboard Bearing Axial Reaction = -1900 lb

* Case Thermally Unstable

NOTE: THERMAL EXCURSION OCCURRED AT 17° AND 21° SUBCOOLING

Table 4

APPENDIX A

UNIT 2 BUILD 4	PN MRS007955-151 BRG #1	SN 8635012 LOAD END

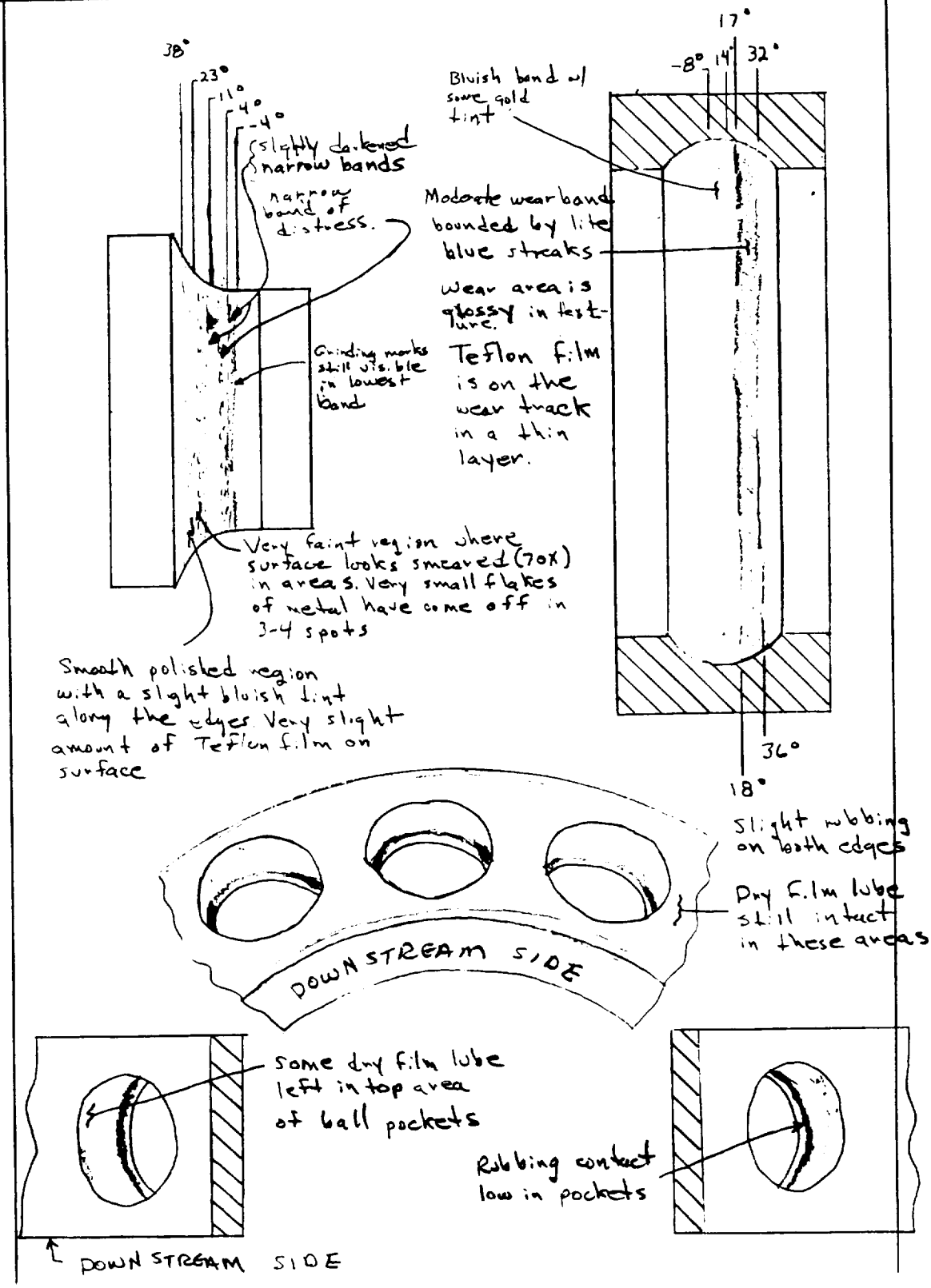

UNIT 2/BUILD 4	BRG # 1	SN 8635012 LOAD END

BALL #	DIA	WEAR
1	.4998	0
2	.4997	↓
3	.4997	
4	.4997	
5	.4997	
6	.4996	
7	.4996	
8	.4996	
9	.4996	
10	.4995	
11	.4997	
12	.4996	
13	.4997	

Balls are smooth, slightly cloudy appearance, still shiny. No wear marks.

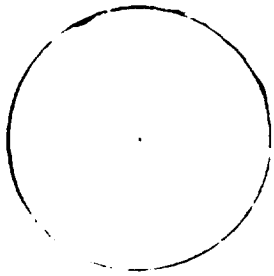

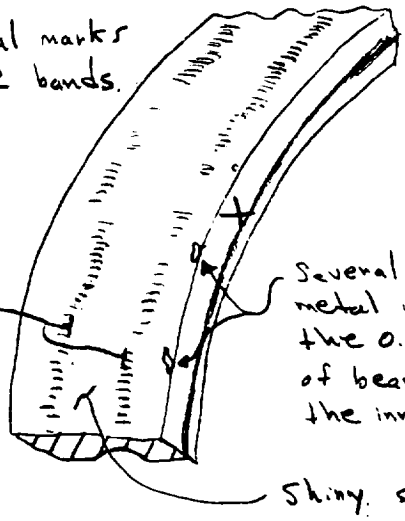

Very faint axial marks 360° around in 2 bands.

1 mm wide spring mark 360° around

Brownish 'stain' in a 90° arc on O.R. Dry film residue from carrier.

Several small flakes of metal were clinging to the O.R. due to magnetism of bearing. Possibly from the inner race.

Shiny silver outer race O.R., No solid film lube on this bearing O.R. or I.R.

UNIT 2 / BUILD 4	PN R0014629-31 BRG #2	SN 8641574 LOAD END

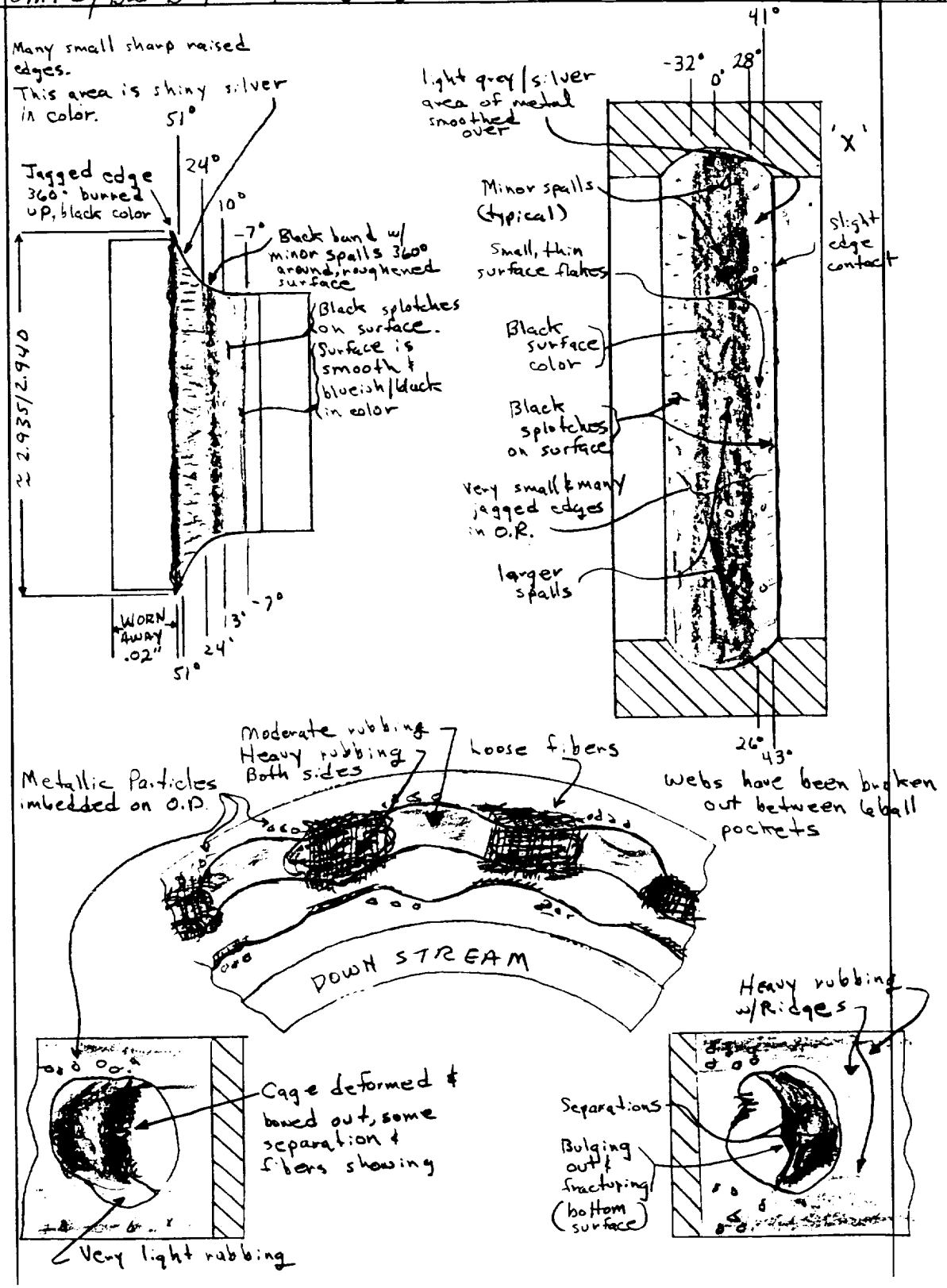

UNIT 2/BUICK 4	BRG #2	SN 8641574

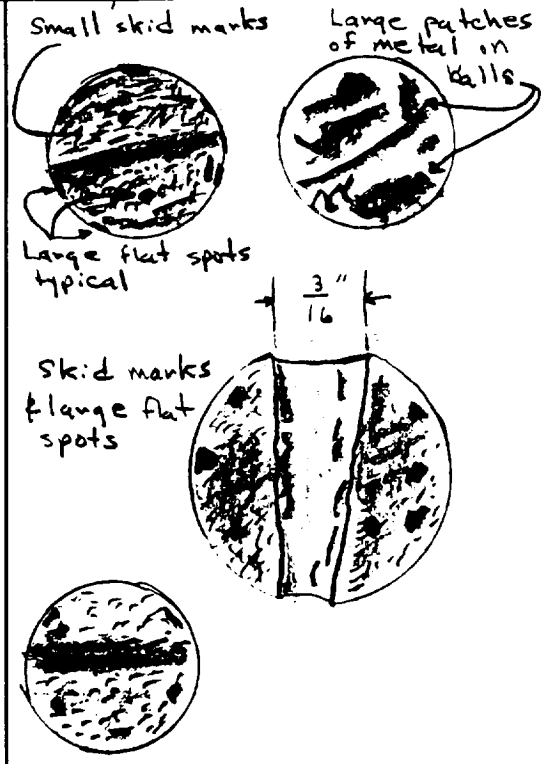

BALL #	DIA	WEAR*
1	.4750	.0248
2	.4558	.0440
3	.4865	.0133
4	.4764	.0234
5	.4866	.0132
6	.4864	.0134
7	.4818	.0180
8	.4741	.0257
9	.4845	.0153
10	.4854	.0144
11	.4744	.0254
12	.4632	.0366
13	.4869	.0129

* Δ FROM AVG OF .4998 NEW SIZE

All balls have blackened surface, Some have brownish hue on the surface. All balls are out of round with flat spots scattered around. Material is deformed and smeared. Some balls have metal adhered onto the surface

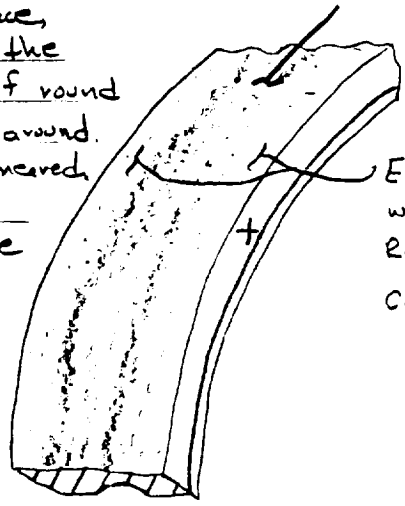

UNIT 2/BULLO 4	PN R0014629-51 BRG #3	DRIVE END SN 8621649

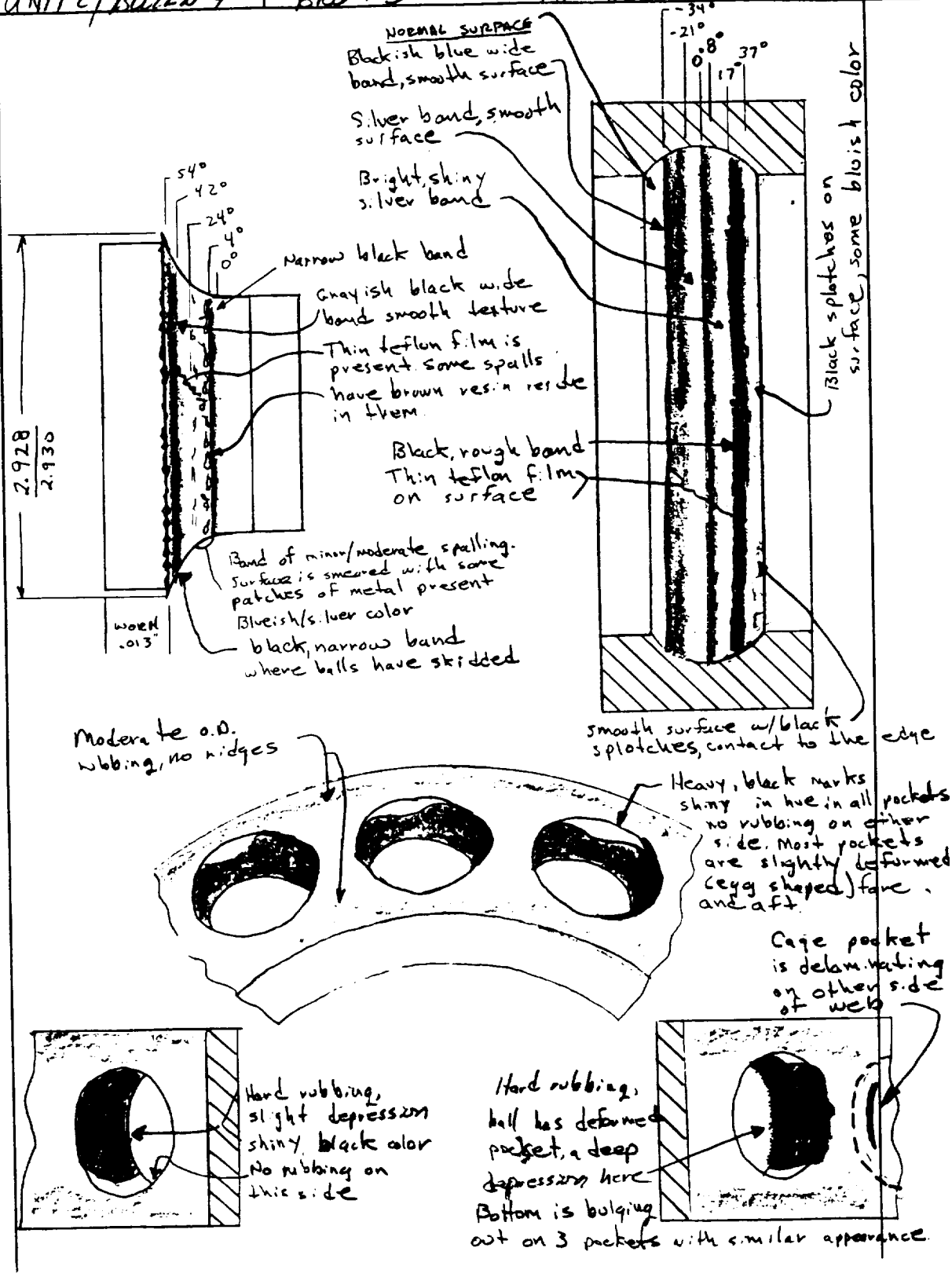

UNIT 2 BALL 04	BRG #3	SN 8621649

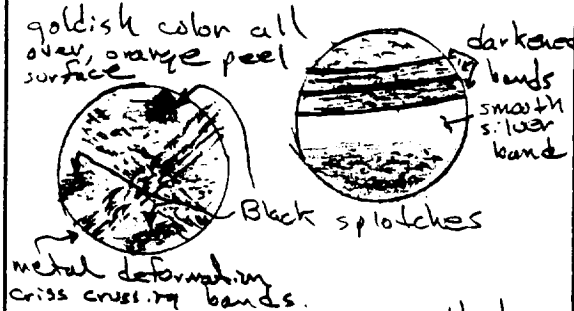

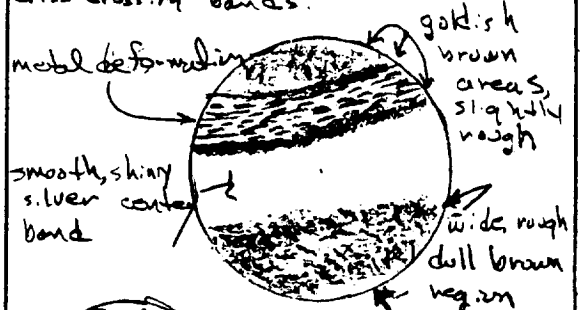

BALL #	DIA	WEAR*
1	.4951	.0047
2	.4939	.0059
3	.4946	.0052
4	.4895	.0103
5	.4951	.0047
6	.4952	.0046
7	.4949	.0049
8	.4950	.0048
9	.4893	.0105
10	.4956	.0042
11	.4957	.0041
12	.4949	.0049
13	.4904	.0094

FROM ANG OF .4998

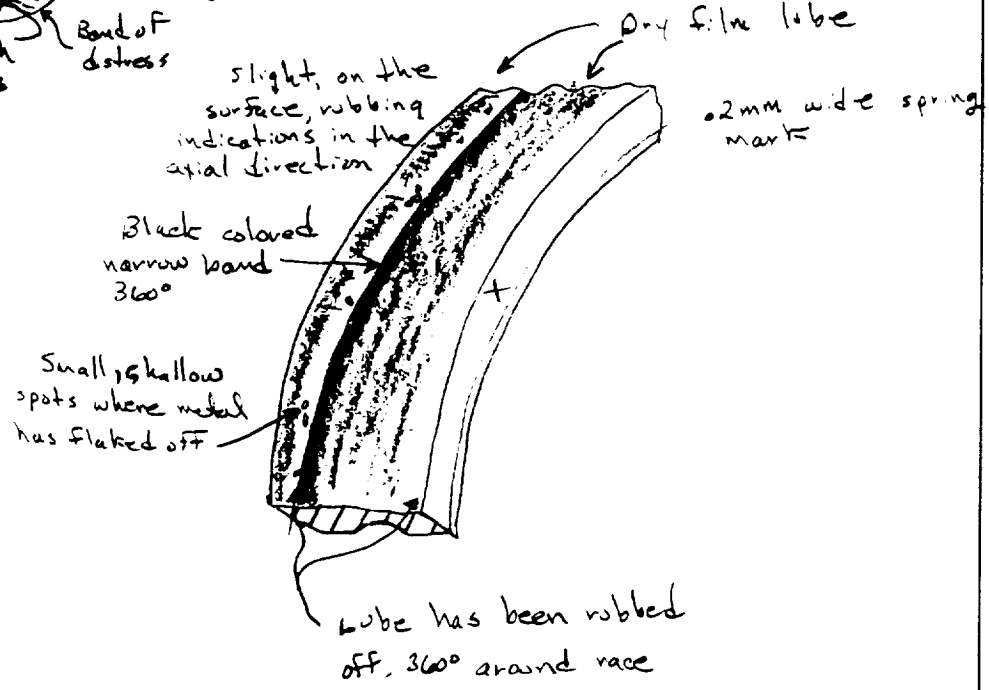

UNIT 2/ BLOCK 4	PN MRS007455-151 BEARING 4	DRIVE END SN 8635060

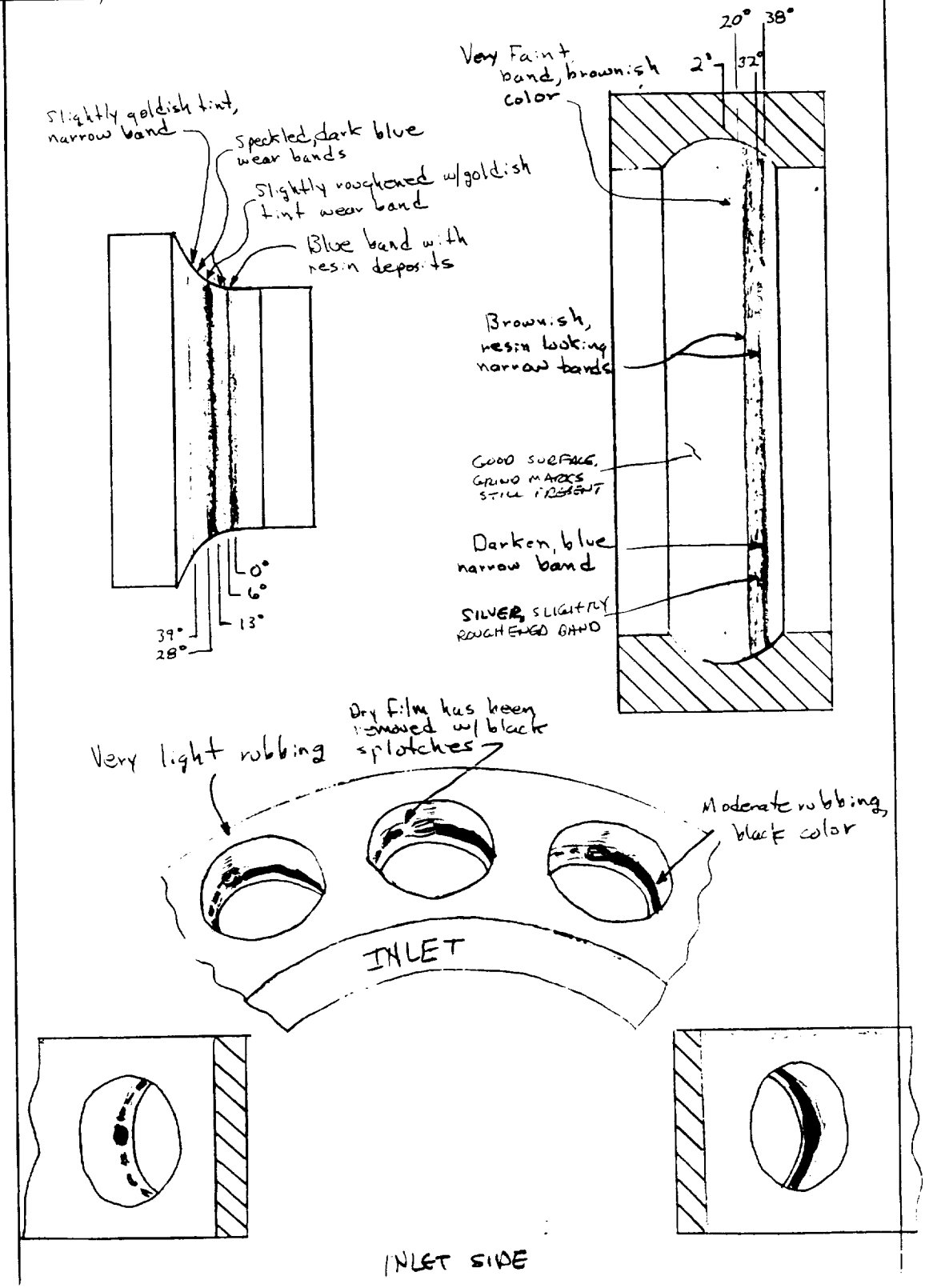

UNIT 2 / BWCM 4	RR6 #4	SN 8635060

BALL #	DIA	WEAR
1	4997	0
2	4998	
3	4997	
4	4998	
5	4998	
6	4997	
7	4996	
8	4997	
9	4997	
10	4997	
11	4996	
12	4996	
13	4997	

Balls are shiny silver w/ dull appearing narrow wear band.